New spintronic superlattices composed of half-metallic compounds with zinc-blende structure

2004 J. Phys.: Condens. Matter 16 S5669

(http://iopscience.iop.org/0953-8984/16/48/025)

INSTITUTE OF PHYSICS PUBLISHING JOURNAL OF PHYSICS: CONDENSED MATTER

J. Phys.: Condens. Matter **16** (2004) S5669–S5676 PII: S0953-8984(04)79451-5

New spintronic superlattices composed of half-metallic compounds with zinc-blende structure

C Y Fong and M C Qian

Department of Physics, University of California, Davis, CA 95616-8677, USA

Received 14 April 2004
Published 19 November 2004
Online at stacks.iop.org/JPhysCM/16/S5669
doi:10.1088/0953-8984/16/48/025

Abstract

The successful growth of zinc-blende half-metallic compounds, namely CrAs and CrSb, in thin film forms offers a new direction to search for novel spintronic materials. By using a well documented first-principles algorithm, the VASP code, we predict the electronic and magnetic properties of superlattices made of these exciting half-metallic materials. Not only are the superlattices constructed with two of the half-metallic compounds (CrAs/MnAs) but also they are modelled to combine with both a III–V (GaAs–MnAs/CrAs/GaAs) and a IV–IV (MnC/SiC) semiconductor. We investigate variable thicknesses for the combinations. For every case, we find the equilibrium lattice constant as well as the lattice constant at which the superlattice exhibits the half-metallic properties. For CrAs/MnAs, the half-metallic properties are presented and the magnetic moments are shown to be the sum of the moments for MnAs and CrAs. The half-metallic properties of GaAs–MnAs/CrAs/GaAs are found to be crucially dependent on the completion of the d–p hybridization. The magnetic properties of MnC/SiC are discussed with respect to the properties of MnC.

1. Introduction

One of the most fundamental characteristics to classify materials is whether they are metallic, semiconducting, or insulating. In 1985, de Groot *et al* [1] predicted that a material can be a half-metal (HM) with electrons with spins polarized in one direction having metallic properties while electrons with opposite spin polarizations show semiconducting behaviour. Half-metallic compounds have attracted much attention recently, in particular in the area of spintronics, i.e., utilization of the electron spin in future electronic devices [2]. In an HM, the spin polarization at the Fermi energy, E_F, is 100%. However, many of the earlier studied half-metallic materials, for example the Heusler alloys, suffer from imperfections in the samples for spintronic applications. NiMnSb is an exception [3]. Recent experiment [4] shows that even when the sample is grown at low temperature, the amounts of disorder are within the tolerance limit to maintain a half-metallic bandstructure. Furthermore, the other potential candidate

for spintronic materials, Mn doped GaAs [5], does not have high enough Curie temperature, T_C (well below 273 K, the room temperature). HMs with simple crystal structure and high T_C are desperately sought. In 2000, Akinaga *et al* [6] predicted half-metallic behaviour for CrAs with simple zinc-blende (ZB) structure and grew it in a thin film form. Their magnetic measurements showed that its T_C is around 480 K. This important work has opened a way to grow a desired new kind of HM with a simple crystal structure that will avoid stoichiometric problems and will have a high T_C. Later, GaSb was also grown in thin film form [7]. Several groups [8–11] have predicted theoretically that many other transition metal compounds with zinc-blende structure will exhibit half-metallic properties. In this paper, we address the issue of whether thin quantum structures, superlattices in particular, made of ZB HM compounds by themselves and with other semiconductors, can possess half-metallic properties. We predict that superlattices of CrAs/MnAs, GaAs–MnAs/CrAs/GaAs and a monolayer of MnC with two different layer thickness of SiC will exhibit half-metallic behaviour. In section 2, we briefly describe the method of calculation. Results for the three kinds of superlattice will be presented in section 3. In section 4, we summarize our results.

2. Method of calculations

We used the well known VASP program developed by Kresse *et al* [12] with the Perdew 91 version of the generalized gradient approximation (GGA) [13] within density functional theory [14]. The cut-off energy, E_{cut}, is 450 eV, which determines the number of plane waves. This cut-off energy gives a convergence of the total energy better than 10^{-2} eV. We use the $11 \times 11 \times N_z$ Monkhorst–Pack [15] mesh to determine the special **k**-points to get the total charge density of the sample. N_z depends on the thickness of the superlattice. Values ranging between 3 and 7 were used. The ultrasoft pseudopotentials of the elements were determined using normal atomic configurations. The density of states (DOS) of the superlattices was calculated using the tetragonal method.

3. Results and discussion

In this section, we present results for three different kinds of superlattice, namely MnAs/CrAs, GaAs–MnAs/CrAs/GaAs, and MnC/SiC. The notation of GaAs–MnAs for the second kind of superlattice means that the region consists of $Ga_{0.5}Mn_{0.5}As$. The lattice constants are optimized and the atoms in the unit cell are fully relaxed.

3.1. CrAs/MnAs

We consider one superlattice of CrAs/MnAs with one one-layer, $(CrAs)_1(MnAs)_1$, and one two-layer superlattice, $(CrAs)_2(MnAs)_2$. In figure 1, we show the superlattice of $(CrAs)_1(MnAs)_1$ in a conventional cell where Cr, Mn, and As atoms are indicated by grey, black, and open circles, respectively. The optimized lattice constant is 5.70 Å, which is close to the average of the optimized lattice constants of constituent CrAs (5.66 Å) and MnAs (5.77 Å) [8]. This lattice constant applies also to the two-layer superlattice. The lattice constant (5.70 Å) of the superlattice differs from the optimized lattice constant of GaAs (5.72 Å) only by 0.3%. This is encouraging because of the possibility of growing these superlattices using GaAs as a substrate.

The total and the projected DOS of $(CrAs)_1(MnAs)_1$ are shown in figure 2. The top panel shows that the sample is an HM. The majority spin channel shows metallic properties, while the minority spin states exhibit semiconducting behaviour. The two panels below demonstrate

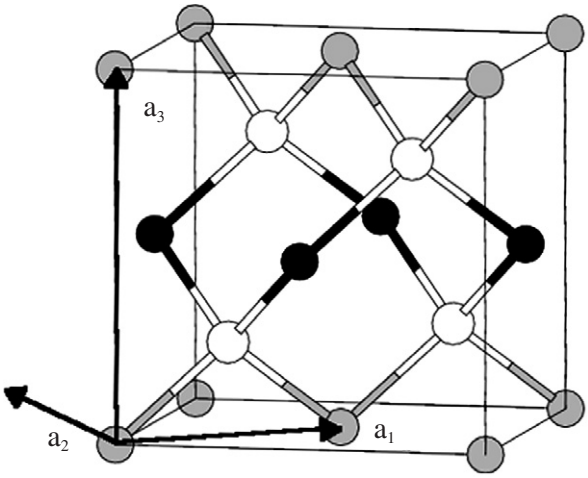

Figure 1. $(CrAs)_1(MnAs)_1$ superlattice conventional cell.

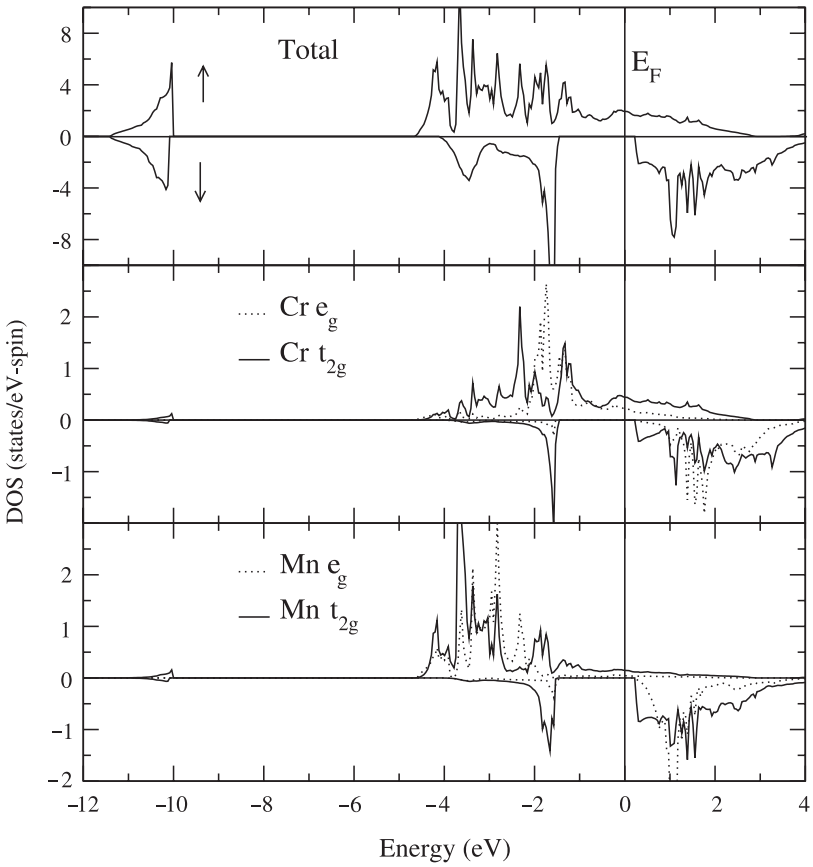

Figure 2. Total and projected density of states of the $(CrAs)_1(MnAs)_1$ superlattice. The material is half-metallic. The positive (negative) values represent majority (minority) spin. The Fermi energy is set to zero.

Table 1. Calculated half-metallic properties of $(CrAs)_1(MnAs)_1$ and $(CrAs)_2(MnAs)_2$ superlattices, and constituent ZB compounds. DOS at E_F in the majority spin channel. E_g is the gap in the minority spin channel, and M is the magnetic moment. All results are per primitive unit cell.

Sample	DOS at E_F (states/eV-spin)	E_g (eV)	M (μ_B)
$(CrAs)_1(MnAs)_1$	1.94	1.65	7.0
$(CrAs)_2(MnAs)_2$	3.47	1.62	14.0
CrAs [8]	0.85	1.85	3.0
MnAs [8]	0.77	1.70	4.0

clearly that the triply degenerate (t_{2g}) Cr-related d states dominate the majority spin states at E_F since these d states are higher in energy than the ones of the Mn atom. Similar results are obtained for $(CrAs)_2(MnAs)_2$. We summarize the half-metallic and other properties of the two superlattices in table 1. The magnetic moments for the superlattices are just the sum of the moments of the constituents. These results do not imply the increase of the saturation magnetization (magnetic moment per unit volume). For ZB CrAs, the saturation magnetization corresponding to the 3.0 μ_B magnetic moment is 572.4 emu cm^{-3} which compares well with the measured value of 559.8 emu cm^{-3}. With the saturation magnetization of MnAs being 763.2 emu cm^{-3}, the value for both superlattices is 672.8 emu cm^{-3}, approximately the average of the two constituents. It is, therefore, not viable to increase the saturation magnetization by growing superlattices.

3.2. GaAs–MnAs/CrAs/GaAs

The specific composition of this second type of superlattice is $(Ga_{0.5}Mn_{0.5}As)_1(CrAs)_2(GaAs)_2$. The sectional view of this superlattice is shown in figure 3. Panel (a) shows that the three regions of the superlattice are separated and viewed along $[\bar{1}10]$. Panel (b) is the superlattice viewed also along $[\bar{1}10]$. We have calculated the electronic properties of the two configurations. The DOS associated with (a) is shown in figure 4(a). The general feature is that the d states of the Mn atoms are more tightly bound than the d states of the Cr atoms. As the layers are separated, the sample becomes a ferromagnetic metal. This is due to the lack of fourfold coordination around the interface atoms, in particular the Cr atoms (figure 3(a)). The hybridization of the Cr d states occurs only with two of the As p states. Therefore, it is not complete. Once the superlattice is formed, every transition metal element has fourfold coordination. The corresponding DOS shown in figure 4(b) demonstrates definitely that the sample is an HM. The Cr t_{2g} states as in $(CrAs)_1(MnAs)_1$ are the dominant contribution of the states at E_F.

Two implications can be inferred from this superlattice.

(i) The presence of the thin GaAs region does not destroy the HM properties. It should facilitate the growth of this type of superlattice on GaAs, in addition to the superlattices made only of CrAs and MnAs.

(ii) This superlattice suggests that, with a limited thickness of GaAs, there is still a possibility to show ballistic transport properties.

We examined the transport properties of this superlattice and identified the channel for ballistic transport [16].

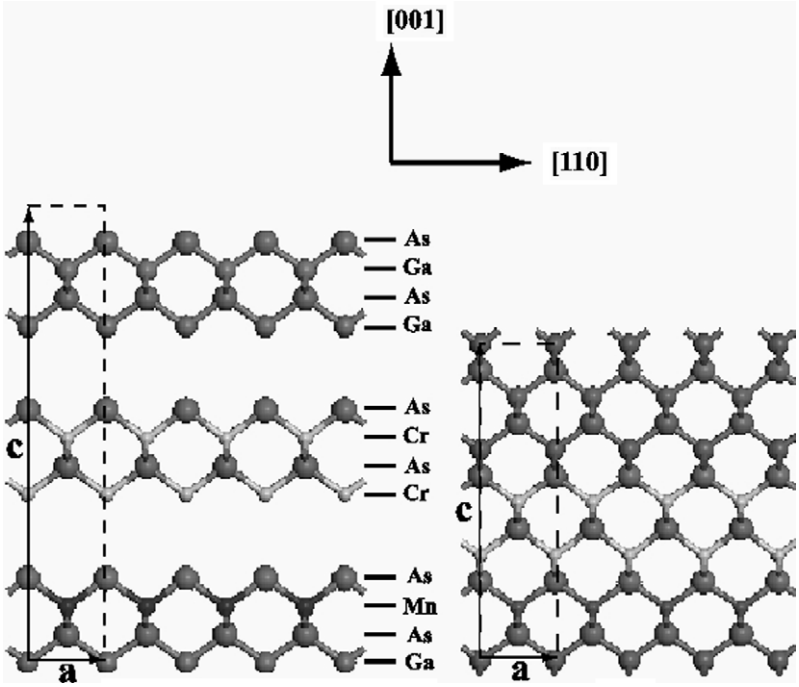

(a) (b)

Figure 3. (a) Separated superlattice; (b) contact superlattice. Both are viewed along **b**, the [$\bar{1}$**10**] direction.

Table 2. Calculated half-metallic properties of $(MnC)_1(SiC)_3$ and $(MnC)_1(SiC)_5$ superlattices. DOS at E_F in the majority spin channel. E_g is the gap in the minority spin channel, and M is magnetic moment. All results are per primitive unit cell.

Sample	Lattice constant (Å)	DOS at E_F (states/eV-spin)	E_g (eV)	M (μ_B)
$(MnC)_1(SiC)_3$	4.55	1.18	1.04	3.0
$(MnC)_1(SiC)_5$	4.60	3.47	1.62	3.0

3.3. MnC/SiC

MnC is a very interesting HM as briefly mentioned in [8]. In figure 5, we show that it has different half-metallic behaviour in two regions of its lattice constant. For large lattice constant ($\geqslant$5.0 Å), the half-metallic properties are similar to the ones shown in figure 2 with a magnetic moment of 3.0 μ_B. When the lattice constant is between 3.6 and 4.28 Å, the majority spin channel exhibits semiconducting behaviour and the minority spin channel has the metallic properties. The magnetic moment of the sample is 1.0 μ_B. For this latter case, however, it is still the majority spin channel that determines the magnetic moment of the sample. The physical origin of the difference has been presented in [17]. By forming superlattices with SiC, we predict that only superlattices having a monolayer of MnC can exhibit half-metallic properties. One case is $(MnC)_1(SiC)_3$ and the other case is $(MnC)_1(SiC)_5$. The optimized lattice constants, the DOS of the majority spin channel at E_F, and the gap of the minority spin states are summarized in table 2. The DOS of $(MnC)_1(SiC)_3$ is shown in figure 6(a). The features are similar to the ones shown in figure 2 and $(MnC)_1(SiC)_5$. A simple argument

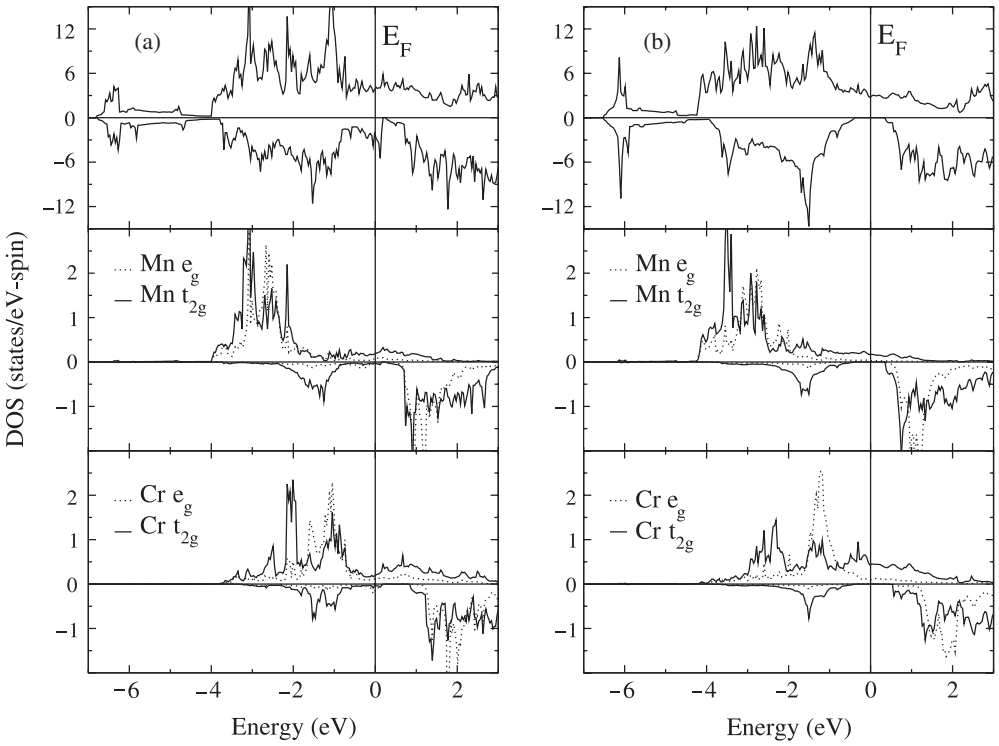

Figure 4. Total and projected density of states of ($Ga_{0.5}Mn_{0.5}As$) (CrAs)(GaAs) (a) in the $c = 4.0\ a_0$ case, and (b) in the $c = 3.0\ a_0$ case. The positive (negative) values represent majority (minority) spin. The Fermi energy is set to zero.

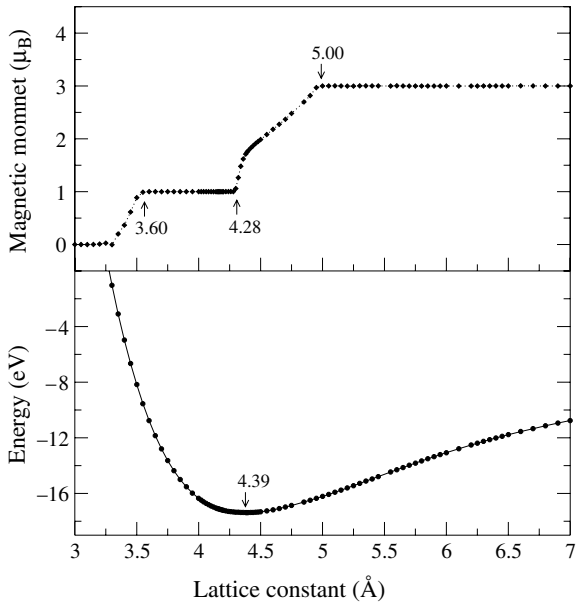

Figure 5. Energy versus lattice constant and Mn magnetic moment versus lattice constant for MnC in the ZB structure.

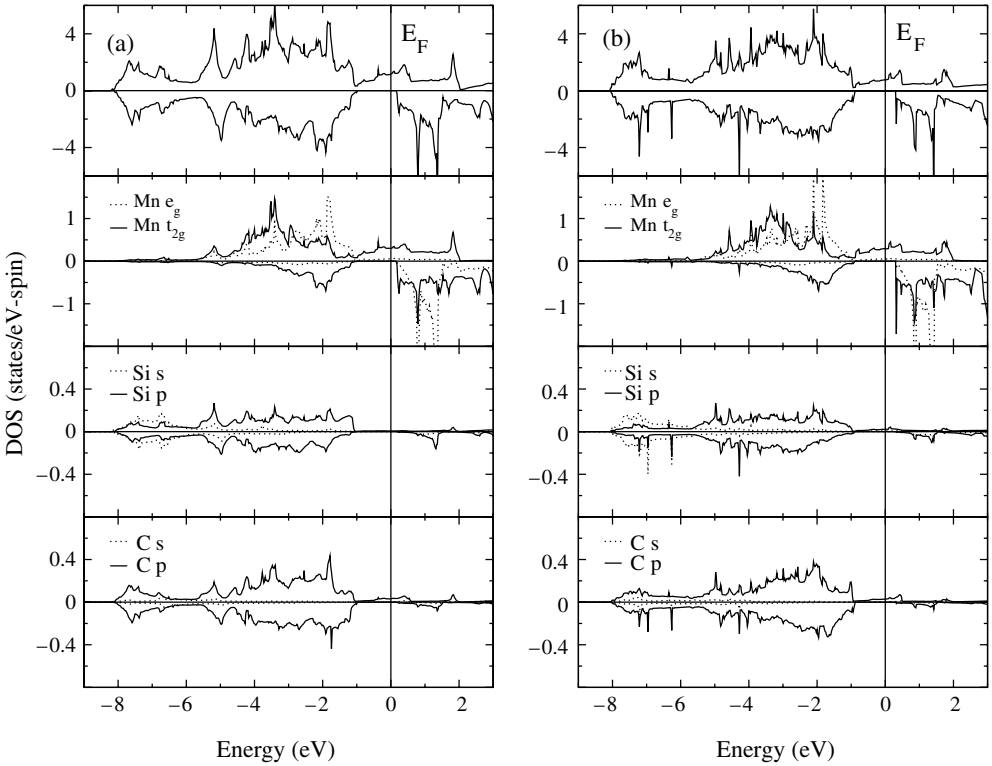

Figure 6. Total and projected density of states of the superlattice (a) $(MnC)_1(SiC)_3$ and (b) $(MnC)_1(SiC)_5$. The positive (negative) values represent majority (minority) spin. The Fermi energy is set to zero.

based on the charge transfer between the anion and the cation can explain the value of the magnetic moment listed in table 2. An Mn atom has seven valence electrons. Four of them are transferred and form bonding states with its nearest neighbour C atoms. This leaves three electrons at the Mn site. The three electrons aligning their spins result in a spin moment of $3/2\ \mu_B$. Consequently, the magnetic moment/unit cell is $3\ \mu_B$. Based on the value of the magnetic moment, the optimized lattice constants for the superlattices are between the optimized values of pure SiC (4.37 Å) and pure MnC (5.0 Å). If SiC is used as a substrate to grow these superlattices, there is at most 5.3% mismatch in lattice constants. This mismatch could cause the stress to be too large for growing MnC on SiC, because SiC is an extremely hard material.

4. Summary

We have used the VASP program to predict that superlattices of $(CrAs)_1(MnAs)_1$, $(CrAs)_2(MnAs)_2$, $(Ga_{0.5}Mn_{0.5}As)_1(CrAs)_2(GaAs)_2$, $(MnC)_1(SiC)_3$, and $(MnC)_1(SiC)_5$ are half-metals. In all these superlatttices (i) the majority spin states exhibit the metallic behaviour and the minority spin states possess semiconducting properties, and (ii) the magnetic moment of each sample is determined by the majority spin states based on the fact that some of the valence electrons of the transition metal elements in a unit cell are transferred to the anions. The remaining electrons of the metallic atoms align their spins, which determines the magnetic

moment per unit cell. We also suggest a promising substrate on which to grow each kind of superlattice, except the superlattices involving MnC.

Acknowledgments

This work is supported by NSF grants Nos INT-9872053 and ESC-0225007, NERSC at Lawrence Berkeley National Laboratory, and the Research Committee at UC Davis.

References

[1] de Groot R A, Muller F M, van Engen P G and Buschow K H 1983 *Phys. Rev. Lett.* **50** 2024
[2] Ball P 2000 *Nature* **404** 918
[3] Schaf J, Dang K Le, Veillet P and Campbell I A 1983 *J. Phys. F: Met. Phys.* **13** 1311
[4] Roy W Van, Wójcik M, Jedryka E, Nadolski S, Jalabert D, Brijs B, Borghs G and Boeck J De 2003 *Appl. Phys. Lett.* **83** 4214
[5] Ohno Y, Young D K, Beschoten B, Matsukura F, Ohno H and Awschalom D 1999 *Nature* **402** 790
[6] Akinaga H, Manago T and Shirai M 2000 *Japan. J. Appl. Phys.* **39** L1118
[7] Zhao J H, Matsukura F, Takamure T, Abe E, Chiba D and Ohno H 2001 *Appl. Phys. Lett.* **79** 2776
[8] Pask J E, Yang L H, Fong C Y, Pickett W E and Dag S 2003 *Phys. Rev.* B **67** 224420
[9] Galanakis I and Mavropoulos P 2003 *Phys. Rev.* B **67** 104417
[10] Zhao Y J, Geng W T, Freeman A J and Delley B 2002 *Phys. Rev.* B **65** 113202
[11] Xie W-H, Xu Y-Q and Liu B-G 2003 *Phys. Rev. Lett.* **91** 037204
[12] VASP, Institut fur Theoretische Physik of the Technische Univeristat, Wien, Austria
Kresse G and Hafner J 1994 *J. Phys.: Condens. Matter* **6** 8245
Kresse G and Furthmuller J 1996 *Phys. Rev.* B **54** 11169
[13] Perdew J P, Burke K and Ernzerhof M 1996 *Phys. Rev. Lett.* **77** 3865
[14] Hohenberg P and Kohn W 1964 *Phys. Rev.* **136** B864
[15] Monkhorst H J and Pack J D 1976 *Phys. Rev.* B **13** 5188
[16] Qian M C, Fong C Y, Pickett W E, Yang L H, Pask J E and Dag S 2004 submitted
[17] Qian M C, Fong C Y and Yang L H 2004 submitted